

# Research on a Micro Cogeneration System with an Automatic Load-Appling Entity

Adrian Chmielewski, Szymon Gontarz, Robert Gumiński,  
Jędrzej Mączak and Przemysław Szulim

**Abstract** The article concerns the testbed research of a micro cogeneration system based on a Stirling engine equipped with an automatic load-applying system. The article presents the influence that the load current has on acceleration of vibration of a micro cogeneration system's body. The research was conducted while using nitrogen as the working gas. Significant number of tests offered the possibility of providing the description of the results in statistical terms while using such measures as kurtosis, coefficient of variation, the asymmetry coefficient as well as the probability density function. The research offers the possibility of concluding whether the completed experiment is repeatable as well as for determining the impact that selected load changes have on acceleration of the micro cogeneration system's vibration.

**Keywords** Automation • Stirling engine • Vibration acceleration • Standard deviation • Measurement

---

A. Chmielewski (✉) · S. Gontarz · R. Gumiński · J. Mączak · P. Szulim  
Faculty of Automotive and Construction Machinery Engineering,  
Institute of Vehicles, Warsaw University of Technology,  
84 Narbutta St, Warsaw, Poland  
e-mail: a.chmielewski@mechatronika.net.pl

S. Gontarz  
e-mail: Szymon.Gontarz@simr.pw.edu.pl

R. Gumiński  
e-mail: rgumin@simr.pw.edu.pl

J. Mączak  
e-mail: jma@mechatronika.net.pl

P. Szulim  
e-mail: p.szulim@mechatronika.net.pl

## 1 Introduction

The paper presents the research related of a micro cogeneration system based on a Stirling engine. This paper presents the influence that loads (with a value of 7, 29, 50, 73 and 93 % of the maximum load) have on acceleration of vibration of a Stirling engine's body in three mutually perpendicular directions.

The tests and the analysis of their results enabled determination of the influence exerted by the analyzed parameters which accompany the system's operation [1–21].

The paper analyzes the repeatability of the obtained values of the body's acceleration in three mutually perpendicular directions while using statistical measures (the average value, the standard deviation of kurtosis, skewness and coefficient of variation as well as the probability density function).

## 2 Presentation of the Testbed with an Automatic Measuring System

The laboratory testbed used for conducting the tests was described in detail in [1, 16]. The experimental data obtained during the research was subjected to analysis while using the statistical measures for the recorded parameters of acceleration of the body's vibration (Fig. 1) in the following directions:  $x$  (parallel to the axis of the cylinders),  $y$  (parallel to the axis of the shaft) and  $z$  (perpendicular to the plane formed by the axis of the shaft).

The system used for applying the loads was constructed while relying on a programmable source of electrical current which is described and presented in detail in [1].

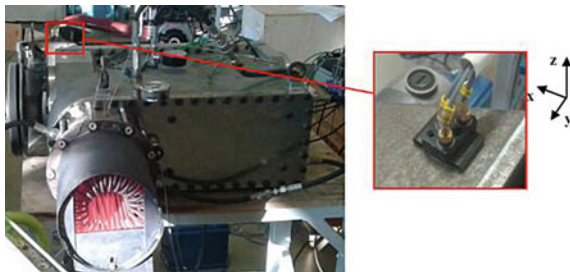


**Fig. 1** Picture of the testbed with a tri-axle vibration acceleration sensor (for capturing vibration of the body)

### 3 Testbed Research

#### 3.1 Results of the Testbed Research

The obtained data was subjected to analysis while using the statistical measures (described in detail in [1] for the recorded parameters) of vibration acceleration in three mutually perpendicular directions. The presentation of the results of the analyses has been restricted to five load values applied to the micro cogeneration system (5, 29, 50, 73 and 93 % of the maximum load).

The further part of the article presents the time runs for the load values ranging from 7 to 93 % of the maximum load for the following items: vibration acceleration in respective directions:  $x$  (Fig. 2a),  $y$  (Fig. 2b),  $z$  (Fig. 2c) as well as their statistical measures.

As expected, the highest acceleration values occur in the direction  $x$ , which is associated with the motion of the piston-crank system. The highest value of the acceleration occurs for the load of 50 %, and in the case of positive acceleration it is  $a_{x\max 29\%} = 33.08 \text{ m/s}^2$  (Fig. 2a) while in the case of negative acceleration it is lower and it has the value of  $a_{x\min 50\%} = -30.8 \text{ m/s}^2$ . For the direction  $x$  the values of vibration acceleration decrease for loads higher than 50 %, and for the load of 93 % they do not exceed  $26.2 \text{ m/s}^2$ .

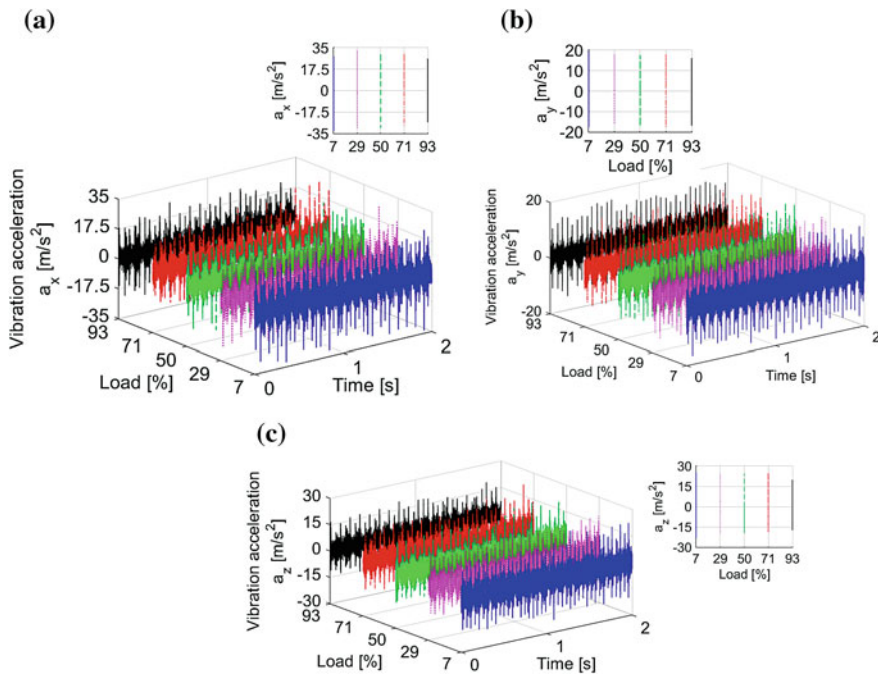


Fig. 2 Vibration acceleration signal curves for directions  $a_x$  (a),  $a_y$  (b) and  $a_z$  (c)

Figure 2b presents the change of vibration acceleration  $a_y$  in the direction y for loads ranging from 7 to 93 % of the maximum load. The highest acceleration value occurred for the load of 7 %, with the maximum value being  $a_{y\max 7\%} = 19.8 \text{ m/s}^2$  for positive acceleration (Fig. 2b). In the case of negative acceleration, the value was higher and amounted  $a_{y\min 7\%} = -17.67 \text{ m/s}^2$ .

Values of vibration acceleration for the direction y decreased as the load increased and they did not exceed  $16.15 \text{ m/s}^2$  for 93 % of the maximum load.

Figure 2c presents the changes of vibration acceleration for loads ranging from 7 to 93 % of the maximum load. The highest value of vibration acceleration was recorded for the positive load of 7 % and amounted  $a_{z\max 7\%} = 25.47 \text{ m/s}^2$  (Fig. 2c), while the lowest value was recorded for the load of 93 % ( $a_{z\min 93\%} = 19.85 \text{ m/s}^2$ ).

The values of vibration acceleration for this direction decrease as the load increases and in the case of the load of 93 % they do not exceed  $20 \text{ m/s}^2$ .

Figure 3a presents the graphs showing the standard deviation for vibration acceleration  $a_x$ , while the values of statistical measures are presented in Table 1. The analysis of graph Fig. 3a and the analysis of the figures found in Table 1 demonstrate that the standard deviation  $\sigma_{ax}$  from the mean value  $\mu_{ax}$  decreases as the load increases. The decreasing standard deviation values for the growing load affect the nature of the growing and positive value of mean kurtosis  $\mu_{Kax}$  (Fig. 3b and Table 1). The distribution is more concentrated than normal (with smaller scatter of the results) It should be also stressed that the scatter of kurtosis for the

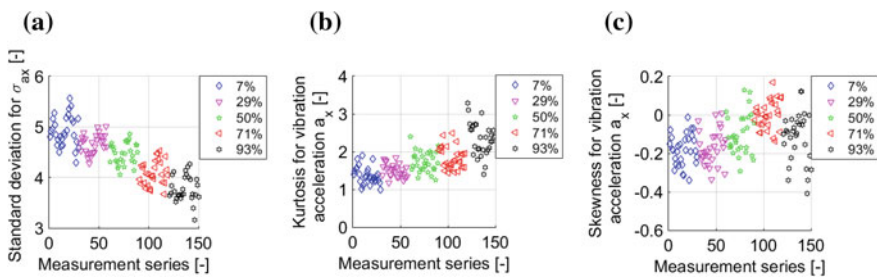


**Fig. 3** Diagrams showing respective measurement values: **a** standard deviation, **b** kurtosis, and **c** skewness for acceleration in the direction x

**Table 1** Test results for vibration acceleration  $a_x$

Load (%)	$\mu_{ax}$	$\sigma_{ax}$	$CV_{ax}$	$\mu_{Kax}$	$\sigma_{Kax}$	$CV_{Kax}$	$\mu_{SKEax}$	$\sigma_{SKEax}$	$CV_{SKEax}$
7	4.913	0.301	0.061	1.364	0.229	0.168	-0.183	0.082	-0.447
29	4.673	0.188	0.040	1.501	0.179	0.119	-0.169	0.089	-0.528
50	4.466	0.210	0.046	1.735	0.270	0.155	-0.101	0.105	-1.045
71	4.086	0.239	0.059	1.826	0.293	0.161	-0.001	0.074	-242.61
93	3.778	0.252	0.067	2.335	0.442	0.189	-0.119	0.130	-1.094

acceleration in the direction x is decreasing, and it decreases as the load increases (from 7 to 93 %).

The mean value of skewness  $\mu_{SKEax}$ , the scatter around the mean value  $\sigma_{SKEax}$  as well as the coefficient of variation  $CV_{SKEax}$  (Fig. 3c and Table 1) grow along with the increase of the system's load.

Figure 4a presents the graphs showing standard deviation for acceleration in the direction y along with the detailed numerical values which are shown in summary Table 2. Analysis of graph Fig. 4a and of the values found in Table 2 show that as the load increases above 7 %, the standard deviation  $\sigma_{ay}$  from the mean value of  $\mu_{ay}$  also increases. It is also the coefficient of variation  $CV_{ay}$  that increases. Growth of the load causes increase of the standard deviation, leading to growth of the positive mean value of kurtosis  $\mu_{Kp}$  (Fig. 4b and Table 2). It is worth adding that the mean value of kurtosis is positive, which means that the distribution is more concentrated than normally (smaller scatter of the results). It should be also stressed that the scatter of kurtosis for the acceleration a is decreasing and it decreases along with the growth of the load (from 7 to 93 %), which is indicated by the decreasing value of  $CV_{Kay}$  coefficient of variation (Table 2).

While analyzing the values of skewness for the acceleration in the direction y (Fig. 4c and Table 1.) one may notice that there occurs right-hand side asymmetry whose mean value  $\mu_{SKEay}$  grows along with the growth of the load (Table 1.) while the standard deviation  $\sigma_{SKEp}$  and the coefficient of variation  $CV_{SKEay}$  are nearly constant

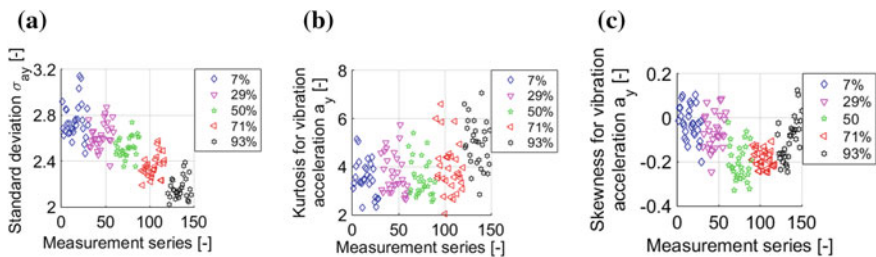


**Fig. 4** Diagrams: **a** standard deviation, **b** kurtosis, and **c** skewness for acceleration in the direction  $a_y$

**Table 2** Test results for vibration acceleration  $a_y$

Load (%)	$\mu_p$	$\sigma_p$	$CV_p$	$\mu_{Kp}$	$\sigma_{Kp}$	$CV_{Kp}$	$\mu_{SKEp}$	$\sigma_{SKEp}$	$CV_{SKEp}$
7	1.187	0.011	0.008	-1.464	0.016	-0.011	0.262	0.021	0.079
29	1.182	0.015	0.013	-1.464	0.017	-0.011	0.266	0.021	0.078
50	1.183	0.016	0.013	-1.472	0.018	-0.012	0.261	0.023	0.088
71	1.179	0.019	0.017	-1.472	0.017	-0.011	0.275	0.022	0.080
93	1.174	0.025	0.022	-1.483	0.014	-0.009	0.270	0.021	0.078

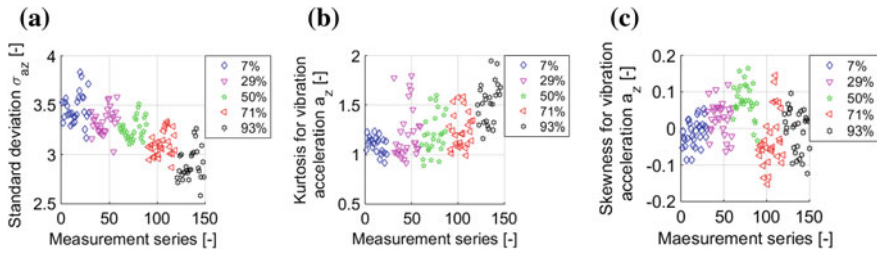


**Fig. 5** Graphs: **a** standard deviation, **b** kurtosis, and **c** skewness for the acceleration in the direction  $a_z$

Figure 5 presents the graphs showing standard deviation (Fig. 5a), kurtosis (Fig. 5b) and skewness (Fig. 5c) for the value  $a_z$  of acceleration in the direction z as the acceleration increases from 7 to 93 % of its maximum value. As the load increases, the mean value of standard deviation  $\mu_{a_z}$  (Table 3) decreases. It is also the mean value of kurtosis (Fig. 5b) that increases and it is positive.

The mean value of skewness  $\mu_{SKEu}$  is positive for the loads of 29 and 50 %, and it is negative for the remaining values of the load, while the standard deviation of skewness,  $\sigma_{SKEu}$ , increases for all load values (Table 3).

Figure 6 shows the influence that the load current has on the value of the probability density function for accelerations in three mutually perpendicular directions.

The results of the examination and the analyses demonstrate that as the load applied to the system grows, so does the value of the probability density function for accelerations in all directions (Fig. 6a–c), which means that the probability of occurrence of a value close the modal value increases along with the growth of the load.

The highest value of the probability density function exists for the acceleration in the direction y for a load equal to 93 % of the maximum load.

**Table 3** Test results for vibration acceleration  $a_z$

Load (%)	$\mu_z$	$\sigma_z$	$CV_z$	$\mu_{Kz}$	$\sigma_{Kz}$	$CV_{Kz}$	$\mu_{SKEz}$	$\sigma_{SKEz}$	$CV_{SKEz}$
7	3.464	0.156	0.045	1.102	0.086	0.078	-0.012	0.036	-3.012
29	3.339	0.126	0.038	1.213	0.260	0.215	0.029	0.045	1.555
50	3.260	0.106	0.033	1.208	0.200	0.166	0.077	0.047	0.608
71	3.103	0.121	0.039	1.241	0.177	0.143	-0.032	0.075	-2.376
93	2.896	0.160	0.055	1.524	0.205	0.134	-0.006	0.058	-9.027

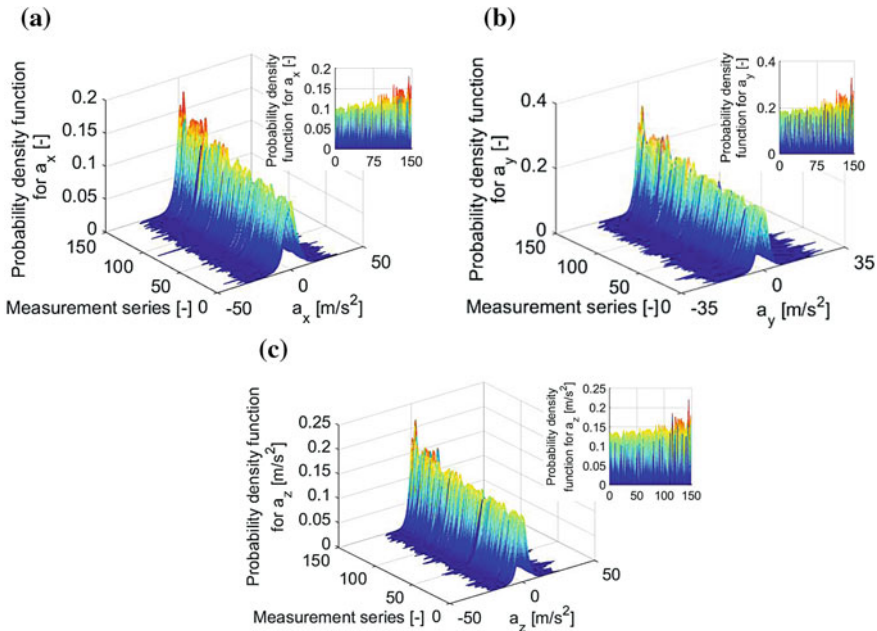


**Fig. 6** Graphs showing the probability density function for acceleration of vibration in respective directions: **a** in direction x, **b** in direction y, **c** in direction z

## 4 Conclusions

Use of statistical measures enabled interpretation of recurrence of results of measurements for a conducted series of measurements. The probability density function has been used to illustrate the probability of occurrence of specific values of acceleration of the engine body’s vibration in the three mutually perpendicular directions. What should also be stressed is that as the load on the system increased, so did the values of the probability density function for acceleration of the engine body’s vibration in all the directions (there occurred smaller standard deviation from the mean value and broader variability range). Based on the conducted research and analyses, one can state that the obtained results are recurrent.

It is extremely important from a cognitive point of view to note that as the system’s load increased from 7 to 93 % of the maximum load, the vibration acceleration in all directions had lower values, which means that vibration acceleration decreased as the load on the micro cogeneration system increased. The reason was the longer work cycle which was accompanied by decrease of crankshaft’s rotational speed. It is also worth noting that as the load increased from 7 to 93 %, the density probability functions achieved higher values, which is indicative of bigger recurrence and predictability of operation of such a system.

In no direction had the vibration acceleration exceeded the value of 3.4 g, nonetheless it is worth noting that the highest values of vibration existed in the direction which is parallel to the axis of the cylinders (direction x), with vibration coming from the movement of the piston-crank system. It should be added that the highest values of vibration acceleration occurred when the pistons were in their extreme positions while the working liquid (gas) was forced between the heat exchangers (the process is described in detail in [3, 6, 13, 14]).

The conducted research offers grounds for concluding that there exists a possibility of diagnosing the level of load of a micro cogeneration system by looking at the vibration acceleration trends. Decrease of vibration acceleration is indicative of more load being applied to a system, which indicates a greater repeatability and predictability of the work of such a system (the growing value of the probability density function for vibration acceleration). The research shows that in the case of bigger workloads (which correspond to higher efficiency), the micro cogeneration systems demonstrate lower values of vibration acceleration, which is very important for users of such systems.

## References

1. Chmielewski, A., Gontarz, S., Gumiński, R., Mączak, J., Szulim, P.: Research study of the micro cogeneration system with automatic loading unit. *Advances in Intelligent Systems and Computing*. Springer (2016) (In print)
2. Chmielewski, A., Gumiński, R., Radkowski, S.: Chosen properties of a dynamic model of a crankshaft assembly with three degrees of freedom. In: 20th International Conference On Methods and Models in Automation and Robotics (MMAR), IEEE, pp. 1038–1043 (2015), ISBN: 978-1-4799-8700
3. Chmielewski, A., Gumiński, R., Radkowski, S., Szulim, P.: Experimental research and application possibilities of a micro-cogeneration system with a Stirling engine. *J. Power Technol.* **95**(Polish Energy Mix), 14–22 (2015)
4. Szablowski, Ł., Milewski, J., Badyda, K.: Cooperation of energy sources in distributed generation. *Rynek Energii*. **6**(115), 120–131 (2014)
5. Li, T., DaWei, T., Li, Z., Du, J., Zhou, T., Jia, Y.: Development and test of a Stirling engine driven by waste gases for the micro-CHP system. *Appl. Therm. Eng.* **33–34**, 119–123 (2012)
6. Bert, J., Chrenko, D., Sophy, T., Moyne, L.L., Sirot, F.: Simulation, experimental validation and kinematic optimization of a Stirling engine using air and helium. *Energy* **78**, 701–712 (2014)
7. Chmielewski, A., Lubikowski, K., Radkowski, S.: Simulation of energy storage work and analysis of cooperation between micro combined heat and power (mCHP) systems and energy storage. *Rynek Energii* **117**(2), 126–133 (2015)
8. Cinar, C., Karabulut, H.: Manufacturing and testing of a gamma type Stirling engine. *Renew. Energy* **30**, 57–66 (2005)
9. Karabulut, H.: Huseyin, Yucesu S., Cinar C., Aksoy F., An experimental study on the development of a  $\beta$ -type Stirling engine for low and moderate temperature heat sources. *Appl. Energy* **86**, 68–73 (2009)
10. Renzi, M., Brandoni, C.: Study and application of a regenerative Stirling cogeneration device based on biomass combustion. *Appl. Therm. Eng.* **67**, 341–351 (2014)



11. Rogdakis, E.D., Antonakos, G.D., Koronaki, I.P.: Thermodynamic analysis and experimental investigation of a Solo V161 Stirling cogeneration unit. *Energy* **45**, 503–511 (2012)
12. Thombare, D.G., Verma, S.K.: Technological development in the Stirling cycle engines. *Renew. Sustain. Energy Rev.* **12**, 1–38 (2008)
13. Xiao, G., Chen, C., Shi, B., Cen, K., Ni, M.: Experimental study on heat transfer of oscillating flow of a tubular Stirling engine heater. *Int. J. Heat Mass Transf.* **71**, 1–7 (2014)
14. Batmaz, I., Ustun, S.: Design and manufacturing of a V-type Stirling engine with double heaters. *Appl. Energy* **85**, 1041–1049 (2008)
15. Chmielewski, A., et al.: Geometrical model of a cogeneration system based on a 1 MW gas engine. *Combust. Engines* **162**(3), 570–577 (2015). ISSN 2300-9896
16. Chmielewski, A., Gumiński, R., Mączak, J., Szulim, P.: Badania układu mikrokogeneracyjnego z silnikiem Stirlinga. Część II. (Research on the micro cogeneration system with a Stirling engine. Part II). *Rynek Energii* **120**(5), 53–60 (2015) (In Polish)
17. Gontarz, S., Szulim, P., Seńko, J., Dybała, J.: Use of magnetic monitoring of vehicles for proactive strategy development. *Transp. Res. Part C* **52**, 102–115 (2015)
18. Chmielewski, A., Gontarz, S., Gumiński, R., Maczak, J., Szulim, P.: Analiza wpływu parametrów eksploatacyjnych na drgania układu mikrokogeneracyjnego. *Przegląd Elektrotechniczny* (2016) (In Print)
19. Chmielewski, A., Gumiński, R., Maciąg, P., Mączak, J.: The use of Fuzzy Logic in the control of an inverted pendulum. *Springer Proceedings in Mathematics and Statistics* (2016) (In Print)
20. Szulim, P., Gontarz, S.: Using the surrounding magnetic field in the diagnosis of BLDC motors. *J. Electr. Eng.—Elektrotechnicky Casopis* (2016) (In Print)
21. Chmielewski, A., Gumiński, R., Mączak, J., Szulim, P.: Model-based research on the micro cogeneration system with Stirling engine. *J. Power Technol.* (2016) (In Print)